World Journal of Chemistry 8 (1): 01-10, 2013
ISSN 1817-3128
© IDOSI Publications, 2013
DOI: 10.5829/idosi.wjc.2013.8.1.1106

Permanent Hard Water Softening Using Cation Exchange Resin in Single and Binary Ion Systems

A.A. Swelam, A.M.A. Salem and M.B. Awad

Department of Chemistry, Faculty of Science (Boys), Al-Azhar University, Cairo, Egypt

Abstract: The present study was undertaken to evaluate the feasibility of strong cation exchange of Resinex^{TM}K-8H (Na^{+}-form) for the removal of Ca^{+2} and Mg^{+2} from synthetic hard water in both single and binary ion systems. The ion exchange behavior of two alkaline-earth metals on the resin, depending on contact time, initial concentration, resin dosage and temperature was studied. The adsorption isotherms were described by means of the Langmuir, Freundlich, Temkin and D-R isotherms. It was found that the Langmuir and Freundlich models are better than the other models. The maximum ion exchange capacity was found to be 0.73 mmol/g for Ca^{+2} and 0.65 mmol/g for Mg^{+2}. The kinetic data were tested using Weber and Morris intraparticle diffusion, pseudo first-order, pseudo second-order and Elovich kinetic models. Kinetic data correlated well with the pseudo-second-order kinetic model, indicating that the chemical adsorption was the rate-limiting step. Various thermodynamic parameters such as Gibbs free energy ($\Delta G°$), enthalpy ($\Delta H°$) and entropy ($\Delta S°$) were also calculated. These parameters showed that the ion exchange of $Ca^{+2}$and Mg^{+2} from aqueous solution was feasible, spontaneous and endothermic process in nature. The activation energy of ion-exchange (E_a) was determined to be 8.79 kJ mol/1 for Ca^{+2} and 8.96 kJ mol/1 for Mg^{+2} according to the Arrhenius equation.

Key words: Missing

INTRODUCTION

Hard waters are characterized by high concentration of calcium and magnesium. Trihalomethanes (THMs) are undesirable byproducts in the water disinfection process by chlorine [1]. Sergio showed that hard waters containing Mg^{+2} and Ca^{+2} are more prone to produce higher THM values than soft waters containing analogous organic compounds [2]. THM promotion of dissolved metal ions follows the order Mg^{+2}>Ca^{+2}. The lower activity of Ca^{+2} can be over-compensated by its higher natural abundance. Permanent hardness can be removed by using a water softener which works on the principle of ion exchange in which calcium and magnesium ions are exchanged with sodium or potassium ions, reducing the concentration of hardness minerals to tolerable levels and thus making the water softer and giving it a smoother feeling [3, 4]. Water softener gradually loses its effectiveness and must be regenerated. This is accomplished by passing a concentrated brine solution through it, causing the above reaction to be reversed. Most of the salt employed in the regeneration process gets flushed out of the system and is usually released into the soil or drainage systems that can have damaging consequences to the environment, especially in arid regions. To avoid the addition of sodium or potassium ions from the softener to the treated water and also the environmental problems of water softeners, developing alternative methods and new materials for hard water softening are important and essential. Among many treatment processes that are currently used for removal of ions from water such as chemical precipitation, evaporation, ion exchange, microbial desalination, adsorption, electrodialysis reverse osmosis and adsorption. Adsorption is the most promising and widely applied method due to its cost effectiveness [5, 6]. Ion exchange is a well-established technique, particularly in water purification, the concentration and removal of metal ions at very low concentrations in chemical process industries. The main advantages of ion exchange over other techniques are the recovery of the metals' value, high selectivity, less sludge volume produced and the ability to meet strict discharge specifications. In addition, the simplicity of ion exchange operation makes it

Corresponding Author: A.A. Swelam, Department of Chemistry, Faculty of Science (Boys), Al-Azhar University, Cairo, Egypt.

attractive to the chemical purification field. In this regard, ion-exchange resins hold great potential for the removal of metals from water and industrial wastewater [7-11].

MATERIALS AND METHODS

Materials: Resinex™K-8H strong acid cation exchange resin were purchased from Jacobi (Swedish carbon company). The mesh size and moisture content were 42-1.25mm and 45-48%, respectively. Calcium and magnesium chloride were of analytical grade and were obtained from Merck. Distilled water (DW) was used to prepare metal ion solutions of known concentrations throughout the study.

Batch Equilibration Method: Prior to use, the resins were washed with HCl and NaOH, converted to Na^+ form and then, the Na^+ form resins decanted and washed with double distilled water to remove possible organic and inorganic impurities sticking to the surface. They were then dried in oven at 60°C to constant weight. For single metal-ion systems, the initial metal concentration ranged from 5 to 20 mmol/l for each Ca^{+2} and Mg^{+2}. The batch experiments were carried out in 100 ml conical flask with stopper. A specific amount of dry resin (0.5g) was added in 50 ml of aqueous Ca^{+2} or Mg^{+2} solutions and then shake for a predetermined period (found out from the kinetic studies) at different temperatures (20, 35 and 50°C) in water bath-cum-mechanical shaker. Afterwards, the concentrations of metal ions were determined. In the binary metal-ion systems, initial concentration of calcium or magnesium was maintained at 20°C and 8 mmol/l to check the influence of competitive ions during the adsorption processes. Competitive adsorption of Ca^{+2} and Mg^{+2} from their binary solution was investigated by following a similar procedure as described above. The uptake of the metal ions, q_e (mmol/g) in single and binary systems was calculated by the difference in their initial and final concentrations. All the tests were carried out in duplicate. Error within ˜5% and the average values were reported. The kinetic experiments were carried out in the range (5-245 min) to determine the effect of contact time with time ranges of 5-245 min. The process of Ca^{+2} and Mg^{+2} removal from an aqueous phase can be explained by using kinetic models and examining the rate-controlling mechanism of the adsorption process such as chemical reaction, diffusion control and mass transfer. Adsorption studies for Ca^{+2} and Mg^{+2} were performed in single and binary ion systems. The applied solid/liquid ratio was 10 g/l. The adsorption capacity in mmol/g of the adsorbent (q_e) and the metal ion adsorption percentage (Ad %) were obtained by Eqs. (1) and (2):

$$qe = \frac{(Co - Ce)v/1000}{W} \quad (1)$$

$$Ads\% = \frac{(Co - Ce)x100}{Co} \quad (2)$$

where C_0 and C_e are the initial and final metal ion concentrations (mmol/l), respectively, V is aqueous phase volume (ml) and W is the weight of adsorbent used (g). The data of isotherms were obtained after an equilibrium time of 24 h. After the equilibrium time, the concentrations were determined by AAS version 6 (Analytik Jena AG Konrad-Zuse-StraBe 1 07745 Jena).

RESULTS AND DISCUSSION

Resinex™K-8H was studied in removal of Ca^{+2}, Mg^{+2} from aqueous solution under different experiment conditions such as contact time, initial concentrations, resin dosage and temperature. The experimental results and the relevant observations are discussed in the following sections.

Effect of Contact Time on Removal of Ca^{+2}, Mg^{+2} in Single and Binary System: Fig. 1 shows the effect of contact time on the removal of Ca^{+2}, Mg^{+2} from aqueous solution in single and binary system by Resinex™K-8H. It is clear that the uptake of Ca^{+2}, Mg^{+2} increased with the lapse of time. The percentage of metal ions adsorbed increased rapidly during a few minutes at first and then increased slowly until the equilibrium state was reached. Fig. 1 revealed that 0.73% adsorption was occurred within 155 min for Ca^{+2} and 65% adsorption was occurred within 185 min for Mg^{+2} in single systems. A further increase in contact time had a negligible effect on the percent removal. The initial adsorption rate was very fast may be due to the existence of greater number of resin sites available for the adsorption of metal ions. It results in the amount of adsorbate accumulated on the resin surface increased rapidly. As the remaining vacant decreased, the adsorption rate decreased due to the increase in the repulsive forces between the alkaline-earth metal ions on the surface and those in the liquid phase. Fig. 1 depicts also the adsorption equilibrium data for the binary systems is lower than those from single component system, i.e. the adsorption follows the order q_eCa^{+2}> q_eMg^{+2} > q_eCa^{+2}(Ca^{+2} + Mg^{+2}) > Mg^{+2} (Ca^{+2} + Mg^{+2}). Evidently the exchange capacity of Ca^{+2} was higher than

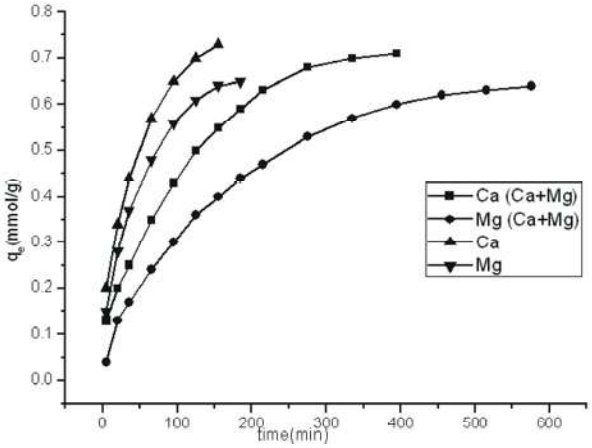

Fig. 1: Effect of contant time on Ca^{+2} and Mg^{+2} sorption in a single and binay system at 293K and 8mmol/l

that of Mg^{+2} and the exchange capacity in the binary-ion systems was lower than the exchange capacity in the single-ion system. This may be ascribed to the influence competitive ions to occupy exchangeable sites on the cation exchange resin and formation of repulsive forces between Ca^{+2} and Mg^{+2} on the solid surface and the liquid phase during the adsorption process [12].

Effect of Resin Dosage: The resin amount is an important parameter to obtain the quantitative uptake of metal ion. The retention of the metals was examined in the relation to the amount of the resin. Fig. 2 shows the removal of Ca^{+2} and Mg^{+2} as a function of resin dosage using Resinex^{TM}K-8H. The resin amount varied from 0.5 to 10 g and equilibrated for 24 h at the initial metal ion concentration of 8 mmol/1 in 50 ml metal ion solution. It is apparent that the increase in the percentage removal with increase in the adsorbent dosage is due to the increase in the number of adsorption sites the equilibrium concentration in liquid phase and contact time required to reach equilibrium decreased with increasing resin dose for a given initial metal concentration. These results were anticipated because increasing adsorbent dose could provide a great of surface area or ion-exchange sites for a fixed initial solute concentration [13]. It may be also concluded that the adsorption capacity was lower at higher adsorbent doses. This may be attributed to overlapping or aggregation of adsorption sites resulting in decrease in total adsorbent surface area available to metal ions and an increase in diffusion path length. It is clear from Fig. 2 that for the quantitative removal of calcium and magnesium in 50ml solution, a minimum resin dosage of 0.5 g for Ca^{+2} Mg^{+2} is required.

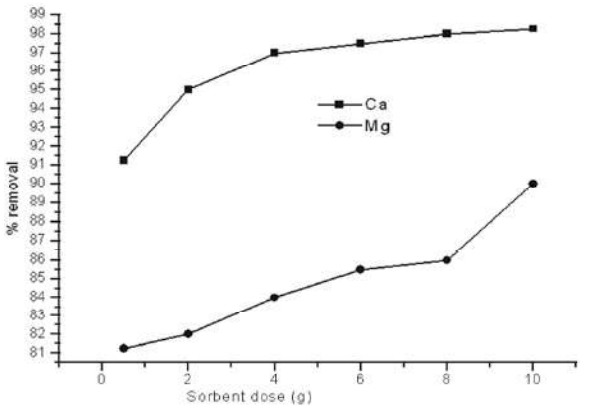

Fig. 2: Effect of sorbent dose on sorption of Ca^{+2} and Mg^{+2}

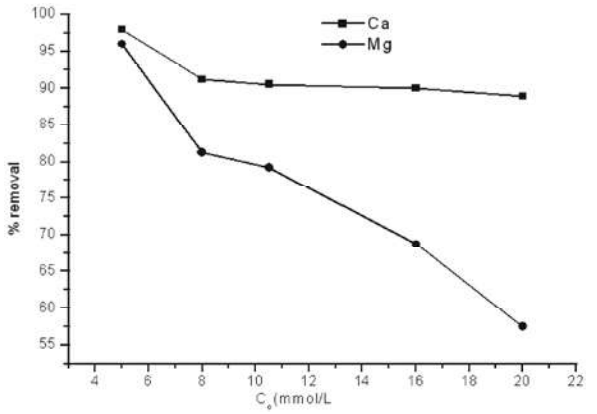

Fig. 3: Effect of initial metal ion concentration of Ca^{+2} and Mg^{+2} sorption

Effect of Metal Ion Concentration: The removal of Ca^{+2} and Mg^{+2} was studied by varying the initial concentration (5, 8, 10.5, 16 and 20 mmol/l) keeping adsorbent dose (0.5g/50ml). The percentage removal decreased with increasing in the initial Ca^{+2} and Mg^{+2} concentrations (Fig. 3). As the calcium and magnesium concentration in the test solution was increased, the adsorption capacity was increased from 0.49 to 0.1.8 mmol/g for Ca^{+2} and from 0.48 to 1.15 mmol/g for Mg^{+2}, respectively. Increasing metal ion concentration increased adsorption capacity for each metal ion, could be attributed to increased rate of mass transfer due to increased concentration of driving force. Also, the results showed that although the equilibrium adsorption increased with increasing metal ion concentration, the extent of this increase was not proportional to the initial metal ion concentration, i.e., a twofold increase in the metal ion concentration did not lead to a doubling of the equilibrium adsorption capacity. This can be explained in terms of the surface area of the substrate on which the competitive

adsorption of ions occurred. The equilibrium time is one of the important parameters for application of economical wastewater treatment.

Ion-Exchange Isotherms: Adsorption isotherms are very powerful tools for the analysis of adsorption process. Adsorption isotherms establish the relationship between the equilibrium pressure or concentration and the amount of adsorbate adsorbed by the unit mass of adsorbent at different temperatures. The Langmuir and Freundlich isotherm models are widely used to investigate the adsorption process. The model parameters can be construed further, providing understandings on adsorption mechanism, surface properties and an affinity of the adsorbent. The Langmuir isotherm [14] is expressed by the relationship:

$$\frac{C_e}{q_e} = \frac{1}{bQo} + \frac{C_e}{Q_o} \quad (3)$$

where C_e is the adsorbate equilibrium concentration (mmol/1) in solution, q_e is the solid phase adsorbate concentration at equilibrium (mmol/g). The constant Q_o gives the theoretical monolayer adsorption capacity (mmol/g) and b is related to the energy of adsorption (J/mmol). The Langmuir isotherm is applied to adsorption on a completely homogenous surface with negligible interaction between adsorbed molecules. The model assumes uniform energies of ion exchange on to the surface and no transmigration of the adsorbate in the plane of the surface. The essential feature of the Langmuir equation can be expressed in terms of a dimensionless separation factor, R_L, defined as:

$$R_L = \frac{1}{1 + bCo} \quad (4)$$

where *b* is the Langmuir constant (J/mmol) and C_0 is the initial concentration (mmol/l). The value of R_L indicates the shape of the isotherm to be unfavorable ($R_L > 1$), linear ($R_L = 1$), favorable ($0 < R_L < 1$), or irreversible ($R_L = 0$). The variation of R_L with the temperature (Fig. 4) were found to be between 0 and 1 for the Ca^{+2} and Mg^{+2} (Table 1) and, therefore, ion exchange of Ca^{+2}, Mg^{+2} are both favorable. It is clear that the Langmuir isotherm model provide an excellent fit to the equilibrium adsorption data, giving correlation coefficients of 1.0 for Ca^{+2} and 0.999 for Mg^{+2}, respectively. Table 1 indicated that lower R_L values of Ca^{+2} than Mg^{+2} indicates that ion exchange is more favorable than Mg^{+2} in this studies. The Freundlich isotherm model is expressed as Freundlich [15]:

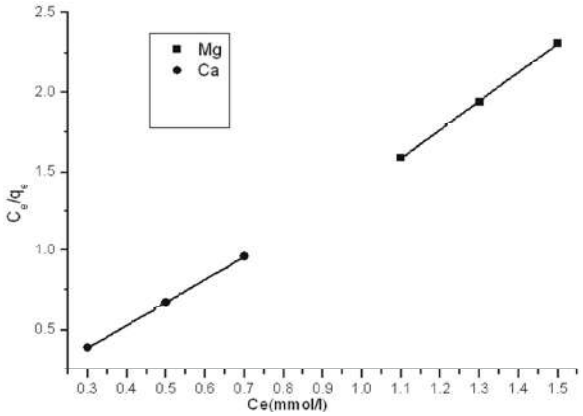

Fig. 4: Langmuir plot for Ca^{+2} and Mg^{+2} adsorption

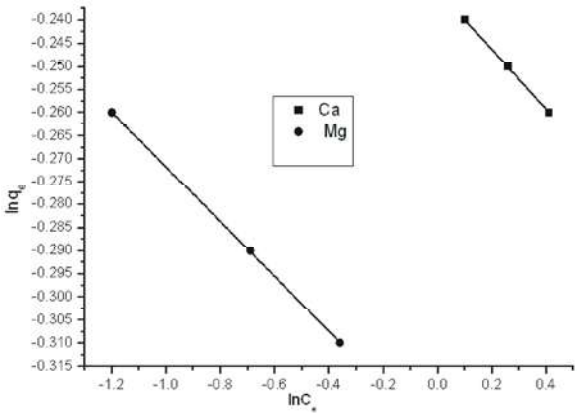

Fig. 5: Freundlich plot for Ca^{+2} and Mg^{+2} adsorption

$$\ln q_e = \ln k_f + (1/n) \ln C_e \quad (5)$$

The constants k_f and n of the Freundlich model are, respectively, obtained from the intercept and the slope of the linear plot of log q_e versus log C_e according to Eq. (5) (Fig. 5). The constant k_f can be defined as an adsorption coefficient which represents the quantity of adsorbed metal ion for a unit equilibrium concentration. Higher values of k_f for Mg^{+2} indicate higher affinity than Ca^{+2}. The slope 1/n is a measure of the adsorption intensity or surface heterogeneity. For 1/n = 1, the partition between the two phases is independent of the concentration. The situation 1/n<1 is the most common and corresponds to a normal L-type Langmuir isotherm, while 1/n>1 is indicative of a cooperative adsorption which involves strong interactions between the molecules of adsorbate. Values of 1/n <1 (0.05946 for Ca^{+2}, 0.06449 for Mg^{+2}) show favorable ion exchange of metals on ion-exchange resin from aqueous solution, respectively. It is found from Table 1 the equilibrium data is fitted well with the Freundlich isotherm model (R^2=1.0 for Ca^{+2} and 0.999 for

Table 1: Adsorption isotherm parameters of Mg^{+2} and Ca^{+2} on Resinex™ K-8H in aqueous solution

	Langmuir parameters				Freundlich parameters		
	Q_0	b	R_L	R^2	1/n	K_f	R^2
Metal ions	mmol/g	L/mg	0.0268	0.999	mg/g	0.79	0.999
Mg^{+2}	0.56	4.54			0.0645		
Ca^{+2}	0.70	36.47	0.0034	1.000	0.0595	0.72	1.000
	Dubinin-Radushkviec parameters				Temkin parameters		
	q_{max}	K'	E	R^2	A	B	R^2
	mmol/g	mol^2kJ^{-2}	kJ/mol	0.974	L/min	J/mol	0.999
Mg^{+2}	0.61	0.0040	11.12		0.0043	0.1299	
Ca^{+2}	0.72	$4.86x10^{-4}$	32.08	0.915	$2.4x10^{-4}$	0.0469	0.970

Mg^{+2}, respectively. Tempkin isotherm equation [16] assumes that the heat of adsorption of all the molecules in the layer decreases linearly with the coverage of molecules due to the adsorbate-adsorbate repulsions and the adsorption of adsorbate is uniformly distributed and that the fall in the heat of adsorption is linear rather than logarithmic. The linearized Tempkin equation is given by Eq. (6):

$$q_e = B_T \ln A_T + B_T \ln C_e \quad (6)$$

where $B_T = RT/b_T$, T is the absolute temperature in K and R is the universal gas constant (8.314 J/mol K). The constant b_T is related to the heat of adsorption, A_T is the equilibrium binding constant (L/min) corresponding to the maximum binding energy. The slope and the intercept from a plot of q_e versus ln C_e (Fig. 6) determine the isotherm constants A_T and b_T (Table 1). To evaluate the adsorption potentials of the adsorbent for adsorbates the Tempkin isotherm constants A_T and b_T are calculated: $2.4x10^{-7}$ L/min and 0.0469 J/mol for Ca^{+2} $4.29x10^{-3}$ L/min and 0.12899 J/mol for Mg^{+2}, respectively (Table 1). The obtained A_T and b_T values indicated a good potential for the two metals. The coefficient of determination (R^2) for Tempkin isotherm model also confirms the better fit of equilibrium data. In order to study the nature of the sorption processes, the D-R isotherm is also verified in the non-linear and linear forms, respectively [17]:

$$q_e = q_{max}\, e^{-k'\varepsilon 2} \quad (7)$$

$$\ln q_e = \ln q_{max} - K'\varepsilon^2 \quad (8)$$

where q_{max} and q_e are the maximum concentration on the solid phase, *i.e.*, ion exchange capacity (mmol/g) and the concentration on the solid at equilibrium (mmol/l), respectively, K' the constant related to the adsorption energy (mol^2kJ^{-2}) and ε is the Polanyi potential ($kJmol^{-1}$) that is defined as follows:

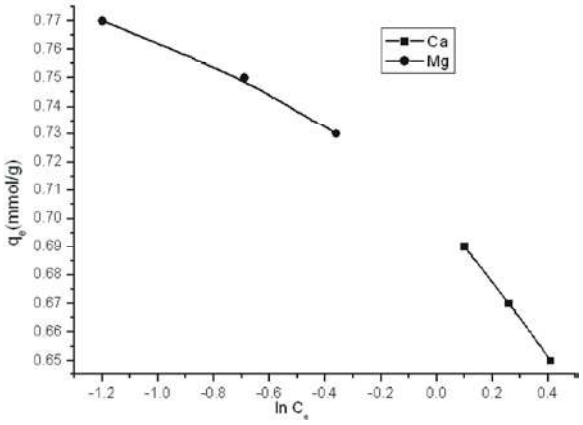

Fig. 6: Temkin plot for Ca^{+2} and Mg^{+2} adsorption

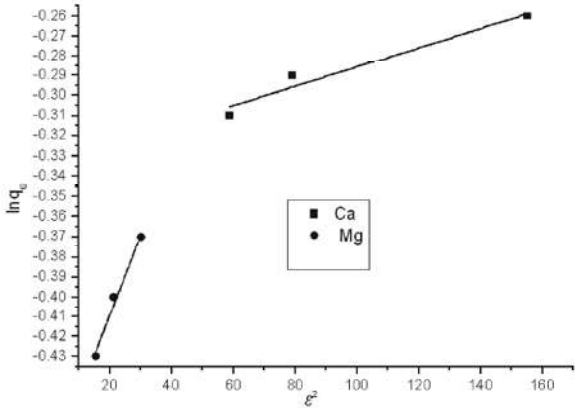

Fig. 7: D-R plot for Ca^{+2} and Mg^{+2} adsorption

$$\varepsilon = RT \ln (1 + 1/ C_e) \quad (9)$$

where C_e is the concentration in the solution at equilibrium (mmol/L) and T is the absolute temperature of the aqueous solution (K). Linear regression analysis using lnq_e and ε^2 (Fig. 7) results in the derivation of q_{max}, K', E and the correlation coefficient (R^2). The correlation coefficient is a statistical measure of how well the data

points fit the regression line. These D-R parameters are presented in Table 1. The mean sorption energy E (kJ/mol), defined as the free energy change when one mole of ion is transferred to the surface of the solid from infinity in the solution, is calculated according to the following equation:

$$E = 1/\sqrt{-2K'} \quad (10)$$

where K' is calculated from the D-R equation. The value of *E* obtained from the slope of the D-R plots is given in Table 1. The magnitude of E is useful for estimating the type of sorption. Calculated mean sorption energy for the sorption of Ca^{+2} and Mg^{+2} on Resinex^{TM}-8H has the value of 32.08 and 11.12 kJ/mol, respectively, which is more than 8 kJ/mol reported by Helfferich,1962 for ion exchange reactions. In the case of E<8.0 kJ/mol, physical forces may affect the sorption mechanism [18]. Overall, the experimental data are found to be fitted well with the Tempkin isotherm model which confirms that the sorption process is chemisorption because of large amount of functional groups on surface and inner of the resin beads. It is also fitted with Langmuir and D-R isotherm model. The results suggested that the adsorption process of calcium and magnesium onto the Resinex^{TM}K-8H beads includes both physisorption and chemisorptions.

Ion-Exchange Kinetics: The two important physicochemical factors for parameter evaluation of the adsorption process as a unit operation are the kinetics and the equilibrium. Kinetics of adsorption describing the solute uptake rate, which in turn governs the residence time of adsorption reaction, is one of the important characteristics defining the efficiency of adsorption. Hence, in the present study, the kinetics of metal removal has been carried out at 293.15-323 K to understand the behavior of this resin. In this study, Lagergren-first-order, pseudo second-order and Elovich equations were used to test the experimental data. The Lagergren-first-order equation is expressed as Lagergren [19]:

$$\ln (q_e - q_t) = \ln q_e - k_1 t \quad (11)$$

Where k_1 (/min) is the rate constant of first-order adsorption, q_e is the amount of metal adsorbed at equilibrium and q_t is the amount adsorbed at time "t". Plotting ln (q_e-q_t) against "t" at 293-323K (Fig. 8) provided first-order adsorption rate constant (k_1) and q_e values from the slope and intercept (Table 2).

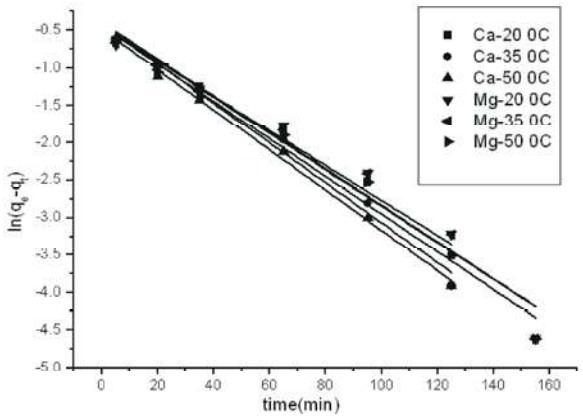

Fig. 8: Psoudo first order kinetic for Ca^{+2} and Mg^{+2} adsorption

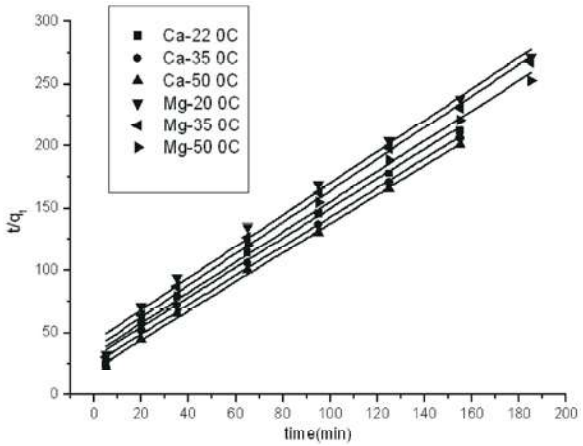

Fig. 9: Psoudo second-order kinetic for Ca^{+2} and Mg^{+2} adsorption

The pseudo-second-order equation is expressed as Yun *et al.* [20]:

$$\frac{t}{q_t} = \frac{1}{k_2 q_e^2} + \frac{t}{q_t} \quad (12)$$

The product $k2q_e^2$ is the initial adsorption rate "h" (mg/g min):

$$h = k_2 q_e^2 \quad (13)$$

The half-adsorption time is time required to uptake half of the maximal amount of adsorbate at equilibrium. It characterizes the adsorption rate as well. In the case of pseudo-second-order process, its value is given by the following relationship:

$$t_{1/2} = 1/k_2 q_e \quad (14)$$

Table 2: Kinetic parameters for Mg^{+2} and Ca^{+2} on Resinex™ K-8H in single and binary aqueous systems

Single system									
		Pseudo first-order model			Pseudo second-order model				
Metal ions	Temp.,K	$q_{e,cal}$ mmol/g	K_1 min^{-1}	R^2	$q_{e,cal}$ mmol/g	K_2 g/mgmin	h mg/gmin	$t_{1/2}$ Min	R^2
Mg^{+2}	293	0.68	0.02443	0.957	0.79	0.03734	0.023	33.86	0.989
	208	0.66	0.02432	0.959	0.80	0.04316	0.027	29.32	0.993
	323	0.64	0.02511	0.978	0.82	0.04451	0.029	27.40	0.993
Ca^{+2}	293	0.64	0.02333	0.987	0.84	0.04558	0.032	26.12	0.989
	208	0.67	0.02666	0.986	0.85	0.05390	0.039	21.83	0.994
	323	0.62	0.02686	0.996	0.86	0.0.6384	0.047	18.35	0.998
					Binary system				
Mg^{+2}	293 K	0.70	0.00754	0.979	0.79	0.00965	0.006	72.43	0.990
Ca^{+2}	293 K	0.77	0.01167	0.964	0.84	0.01643	0.012	103.0	0.979

Single system							
		Intraparticle diffusion model			Elovich model		
Mg^{+2}	Temp.,K	K_{id} $mg/gmin^{0.5}$	C mg/g	R^2	∝ mmol/gmin	B g/mg	R^2
	293	0.04527	0.084	0.967	15.76	6.73	0.975
	208	0.04521	0.107	0.958	13.77	6.69	0.986
	323	0.04528	0.133	0.938	11.88	6.60	0.992
Ca^{+2}	293	0.05314	0.108	0.978	11.43	6.18	0.971
	208	0.05357	0.136	0.959	9.910	6.04	0.984
	323	0.05233	0.178	0.923	8.260	6.02	0.995
				Binary system			
Mg^{+2}	293 K	0.02862	0.018	0.973	53.38	7.00	0.943
Ca^{+2}	293 K	0.03611	0.064	0.969	27.34	6.59	0.930

where k_2 (g/mg min) is the pseudo-second-order rate constant, q_e is the amount adsorbed at equilibrium, $t_{1/2}$ is the half adsorption time and q_t is the amount of metal adsorbed at time "t". Plotting t/q_t against "t" at 293-323K (Fig. 9) provided second order adsorption rate constant (k_2) and q_e values from the slope and intercept (Table 2). Elovich equation [21] is a rate equation based on the adsorption capacity describing adsorption on highly heterogeneous adsorbents. Elovich equation is simplified by assuming $\propto\beta << t$ and by applying the boundary conditions $q_t = 0$ at $t = 0$ and $q_t = q_t$ at $t = t$:

$$q_t = \frac{1}{\beta}\ln(\propto \beta) + \frac{1}{\beta}\ln t \quad (15)$$

where $\propto$ (mg/g min) is the initial adsorption rate and β (g/mg) is the desorption constant related to the extent of the surface coverage and activation energy for chemisorption. The Elovich kinetic constants $\propto$ and β are obtained from the intercept and the slope (Fig. 10), respectively. From the corresponding parameters summarized in Table 2, it is observed that the kinetic behavior of Ca^{+2} and Mg^{+2} sorption onto the resin is more appropriately described by the pseudo second order model because of a much higher correlation coefficient and a much lower standard diversion. The calculated kinetic parameters for pseudo first order, second order and Elovich kinetic models are listed in Table 2. It can be seen that the calculated q_e by second order was more close to the experiment q_e, corroborated the above analysis with the same conclusion. The pseudo second order model was developed based on the assumption that the determining rate step may be chemisorptions promoted by covalent forces through the electron exchange, or valency forces through electrons sharing between sorbent and sorbate, indicating that the sorption of Ca^{+2} and Mg^{+2} on this types of cation exchange resin is mainly the chemically reactive sorption. The sorption process also fit pseudo first order and Elovich kinetic with correlation coefficient more than 0.975 and standard diversion very low. It means that sorption of Ca^{+2} and Mg^{+2} on this type resin there is also physical adsorption. Taking into account that the kinetic results are fitted very well to a chemisorption model, the intraparticle diffusion model was plotted in order to verify the influence of mass transfer resistance on the binding of metal ions to the Resinex™K-8H. The kinetic results were analyzed by the Weber and Morris intraparticle diffusion model [22] to elucidate the diffusion mechanism, which is expressed as:

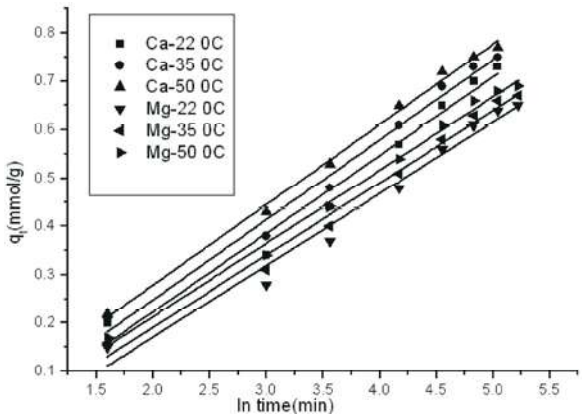

Fig. 10: Elovic plot for Ca^{+2} and Mg^{2} adsorption

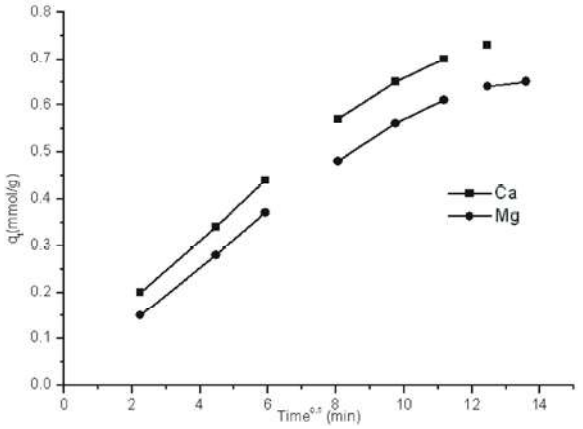

Fig. 11: Weber-Morris model of Ca(ll) and Mg(ll) sorption on Resinex™ K-8H at 293 K

$$q_t = k_{id}t^{1/2} + C \quad (16)$$

The amount of calcium or magnesium adsorbed (q_t) at time (t) was plotted against the square root of time ($t^{1/2}$), according to Eq. (16) and the resulting plot is shown in Fig. 4. Where k_{id} is the intraparticle diffusion rate constant and C is the intercept related to the thickness of the boundary layer. According to Eq. (16), a plot of qt versus $t^{1/2}$ should be a straight line from the origin if the adsorption mechanism follows the intraparticle diffusion process only. However, if the data exhibit multi-linear plots, then the process is governed by two or more steps. It is clear from the Fig. 11 that there are two separate zones: first linear portion (phase I) and second linear part (phase II). The first linear portion (phase I) can be attributed to the immediate utilization of the most readily available adsorbing sites on the adsorbent surface. Phase II may be attributed to very slow diffusion of the adsorbate from the surface site into the inner pores.

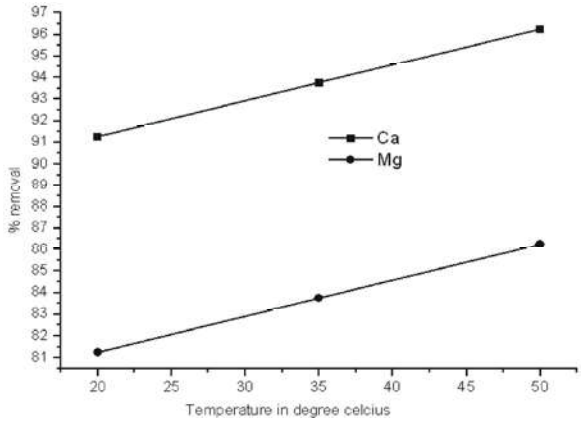

Fig. 12: Effect of temperature on percentage removal of Ca(ll) and Mg(ll) with C_0 = 8 mmol/l

Thus initial portion of calcium and magnesium adsorption by adsorbent may be governed by the initial intraparticle transport of the metal ions controlled by surface diffusion process and the later part controlled by pore diffusion. However, the intercept of the line fails to pass through the origin which may be due to the difference in the rate of mass transfer in the initial and final stages of adsorption (Table 2). Further, such deviation of the straight lines from the origin reveals that the pore diffusion is not the sole rate-controlling step.

Effect of Temperature and Thermodynamic Evaluation of the Process: Temperature parameters can affect the sorption process considerably. So, experiments were made to optimize the favorable temperature to have maximum recovery of alkali-metal ions. Experimental results concerning the effect of temperature on Ca^{+2} and Mg^{+2} metal ions sorption at three temperatures namely, 20, 35 and 50°C are represented as percentage removal of the metal ions versus temperature (Fig. 12). The percentage removal of calcium with initial concentration 8 mmol/l, increased from 91.25 to 96.25 and from 81.25 to 86.25 for magnesium, respectively. These results reveal that an increase in temperature results in an increase in metal ion sorption. The increase in temperature is known to increase the rate of diffusion of metal ions across the external boundary layer and in the internal pores of the resin. According to Monica *et al.* [23] changes in temperature also change the equilibrium capacity of the sorbent for particular sorbate. The increase in sorption percentage may also be due to the acceleration of some originally slow sorption steps or due to the retardation of the processes such as association of ions, aggregation of molecules, ion pairing and complex formation in the

Table 3: Thermodynamic parameters for Mg^{+2} and Ca^{+2} on Resinex™ K-8H

	ΔS	ΔH	E_a		ΔG (kJ/mol)		
Metal ions	(J/mol)	(kJ/mol K)	(kJ/mol)	A	-293	-208	-323
Mg^{+2}	26.41	9.85	8.96	0.31	-2.05	-1.69	-1.26
Ca^{+2}	20.90	62.29	8.79	0.61	-0.10	-1.05	-6.90

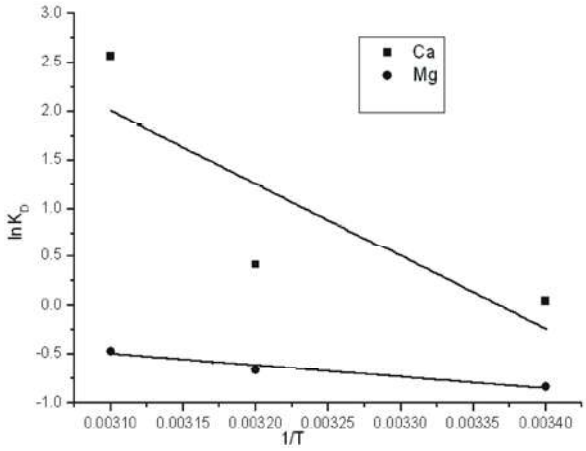

Fig. 13: VantHoff plot for Ca^{+2} and Mg^{+2} adsotption

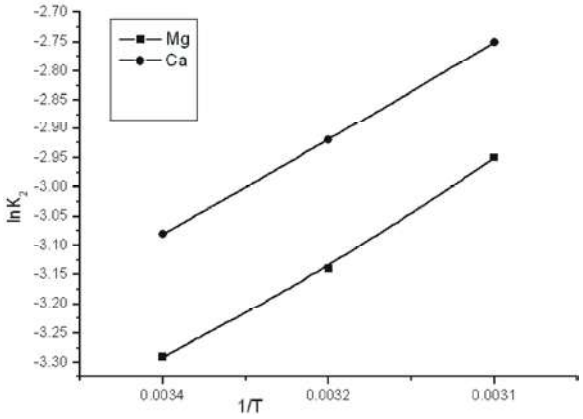

Fig. 14: Arrhenius plot for Ca^{+2} and Mg^{+2} adsorption

system because of thermal agitation. Furthermore, sometime an increase in temperature will reduce the electrostatic repulsion between the surface and the sorbing species, allowing sorption to occur more readily. Results of present temperature study confirm that these materials gave a positive response to an increase in temperature with respect to metal ions sorption. The sorption data obtained from the above study (i.e. effect of system temperature on sorption process) was used to calculate the thermodynamic parameters. Gibbs free energy change (ΔG°), enthalpy change (ΔH°) and entropy change (ΔS°) could be estimated using equilibrium constants changing with temperature [23]:

$$\ln K_D = \frac{\Delta S^0}{R} - \frac{\Delta H^0}{RT} \quad (17)$$

The Gibbs free energy change of the adsorption reaction is given by the following Eq.:

$$\Delta G° = -RT \ln k_D \quad (18)$$

where R is universal gas constant (8.314 J/mol K), T is absolute temperature (K) and $k_D(q_e/C_e)$ is the distribution coefficient. Values of ΔH° and Δ*S*° can be determined from the slope and the intercept of the plot between $\ln k_D$ versus 1/T (Fig. 13). Values of ΔG°, ΔH° and ΔS° along with relation coefficients are given in Table 3. The magnitude of ΔG° decreased with rising of temperature, indicating that the adsorption is favorable at high temperatures. The negative values confirm the feasibility of the process and the spontaneous nature of adsorption of Ca^{+2}, Mg^{+2} on Resinex^{MT}K-8H. From Table 3 it is clear that positive value of ΔH°, suggests the endothermic nature of the adsorption. The positive values of Δ*S*° showed that Ca^{+2} and Mg^{+2} in bulk phase was in a much lower chaotic distribution compared to the relatively ordered surface of adsorbent during the adsorption process. The negative values of ΔG° indicate the spontaneous nature of the adsorption process. In addition, amount of Ca^{+2} and Mg^{+2} absorbed at three different temperatures showed an increase trend with increase in temperature accompanied by increasing entropy suggested that adsorption process was higher favorable at higher temperature.

Activation Energy: Activation energy E_a is determined according to the Arrhenius equation:

$$\ln k_2 = \ln A - E_a/RT \quad (19)$$

where k_2 is the rate constant of pseudo second-order value for the metal adsorption, E_a is the activation energy in kJ/mol, T is the temperature in Kelvin and R is the gas constant (8.314 J/mol K) and A is constant called the frequency factor. Value of E_a can be determined from the slope of $\ln k_2$ versus 1/*T* plot (Fig. 14). The activation energy for the adsorption of Ca^{+2}, Mg^{+2} on Resinex^{MT}-8H

resin was calculated and its value was found to be 8.79 and 8.96 kJ/mol for Ca^{+2} and Mg^{+2} (Table 3), respectively. These values are of the same magnitude as the activation energy of activated chemisorption. It is known that when activation energy is low the rate is controlled by intra-particle diffusion mechanism and hence it can be concluded that process is governed by interactions of physical nature. The positive values of E_a also suggest that rise in temperature favors the adsorption and adsorption process is an endothermic process in nature.

REFERENCES

1. Attias, L., A. Contu, A. Loizzo, M. Massiglia, P. Valente and G.A. Zapponi, 1995. Trihalomethanes in drinking water and cancer: risk assessment and integrated evaluation of available data, in animals and humans. Sci. Total Environ., 171: 61-68.
2. Sergio N., M. Alvaro and H. Garcia, 2009. Ca^{2+} and Mg^{2+} present in hard waters enhance trihalomethane formation. J. Hazard. Mater., 169: 901-906.
3. Zhihui, Y., T. Qia, J. Qu, L.Wang and J. Chu, 2009. Removal of Ca (II) and Mg (II) from potassium chromate solution on Amberlite IRC 748 synthetic resin by ion exchange. J. Hazard. Mater., 167: 406-412.
4. Maryam, A. Tofighy and T. Mohammadi, 2011. Permanent hard water softening using carbon nanotube sheets. Desalination, 268: 208-213.
5. Younggy, K. and B.E. Logan, 2013: Microbial desalination cells for energy production and desalination. Desalination, 308: 122-130.
6. Kristen, S.B. and Z. He, 2013. Water softening using microbial desalination cell technology. Desalination, 309: 32-37.
7. Abdelwahab, O., N.K. Amin and E-S.Z. El-Ashtoukhy, 2013. Removal of zinc ions from aqueous solution using a cation exchange resin. Chem. Eng. Research and Design, 91: 165-173.
8. Dumitru, B. and L. Bulgariu, 2013. Sorption of Pb (II) onto a mixture of algae waste biomass and anion exchanger resin in a packed-bed column; Biores. Technol., 129: 374-380.
9. Karunakaran, M., C.T. Vijayakumar, D. Muthamil Selvan and C. Magesh, 2013. O-Cresol, thiourea and formaldehyde terpolymer - A cation exchange resin. Journal of Saudi Chem. Soc., 17: 1-8.
10. Rajeev, K., M. Kumar, R. Ahmad and M.A. Barakat, 2013. L-Methionine modified Dowex-50 ion-exchanger of reduced size for the separation and removal of Cu (II) and Ni (II) from aqueous solution. Chem. Eng. J., 218: 32-38.
11. Asif, A. K. and S. Shaheen, 2013. Synthesis and characterization of a novel hybrid nano composite cation exchanger poly-o-toluidine Sn (IV) tungstate. Solid State Sci., 16: 158-167.
12. Agrawal, A. and K.K. Sahu, 2006. Separation and recovery of lead from a mixture of some heavy metals using Amberlite IRC 718 chelating resin, J. Hazard. Mater., B133: 299-303.
13. Malkoc, E. and Y. Nuhoglu, 2007. Potential of tea factory waste for chromium (VI) removal from aqueous solutions: thermodynamic and kinetic studies: Sep. Purif. Technol., 54: 291-298.
14. Langmuir, I., 1916. The constitution and fundamental properties of solids and liquids. J. Am. Chem. Soc., 38: 2221-2295.
15. Freundlich, H.M.F., 1906. Uber die adsorption in lasungen. Z. Phys. Chem., 57: 385-470.
16. Temkin, J.M. and V. Pyzhev, 1940. Kinetics of ammonia synthesis on promoted iron, Catalysts Kinetics of ammonia synthesis on promoted iron catalysts: Acta Physiochim, URSS, 12: 217-222.
17. Dubinin, M.M. and L.V. Radushkevich, 1947. Equation of the characteristic curve of activated charcoal. Process Acad. Sci., USSR, 55: 331-333.
18. Helfferich, F., 1962. Ion Exchange. McGraw Hill, New York.
19. Lagergren, S., 1898. Zur theorie der sogenannten adsorption geloster stoffe. K. Sven, Vetenskapsakad. Handl., 24: 1-39.
20. Yun, Z., Y. Li, L. Yanga, X. Ma, L. Wang and Z.F. Ye, 2010. Characterization and adsorption mechanism of Zn^{2+} removal by PVA/EDTA resin in polluted water: J. Hazard. Mater., 178: 1046-1054.
21. Chien, S.H. and W.R. Clayton, 1980. Application of Elovich equation to the kinetics of phosphate release and sorption in soils. Soil Sci. Soc. Am. J., 44: 265-268.
22. Weber, W.J. and J.C. Morris, 1963. Kinetics of adsorption on carbon from solution. J. Sanit. Eng. Div. ASCE, 89: 31-59.
23. Monica, C., S. Mato, G. Gonzalez-Benito, M.A. Uruena and M.T. Garcia-Cubero, 2010. Use of weak cation exchange resin Lewatit S 8528 as alternative to strong ion exchange resins for calcium salt removal: J. Food Eng., 97: 569-573.